Université de Mons
Faculté Polytechnique – Service de Mécanique Rationnelle, Dynamique et Vibrations
31, Bld Dolez - B-7000 MONS (Belgique)
065/37 42 15 – georges.kouroussis@umons.ac.be

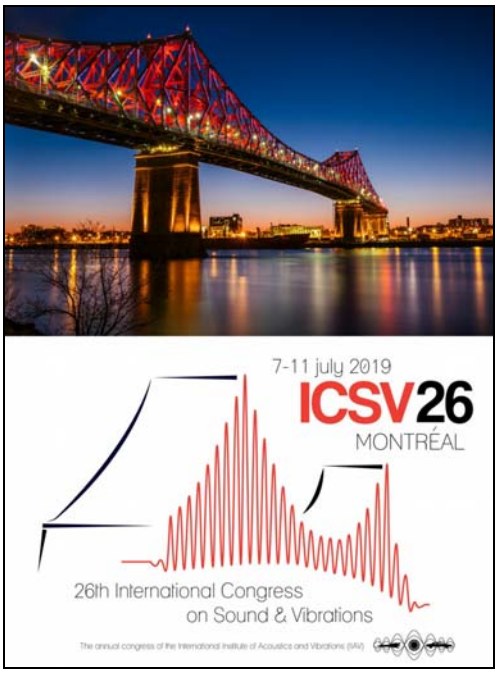

G. Kouroussis, B. Olivier, A. Romero, P. Galv\'in, D. P. Connolly, A FE/BE approach for predicting railway ground vibration generated in urban areas, *Proceedings of the 26th International Congress on Sound and Vibration*, Montréal (Canada) July 7–11, 2019.

26th INTERNATIONAL CONGRESS ON SOUND AND VIBRATION
7-11 July 2019, Montreal

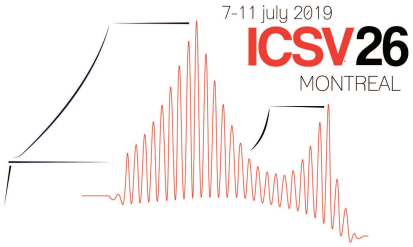

A FE/BE APPROACH FOR PREDICTING RAILWAY GROUND VIBRATION GENERATED IN URBAN AREAS

Georges Kouroussis, Bryan Olivier
University of Mons, Faculty of Engineering, Department of Theoretical Mechanics, Dynamics and Vibrations, Mons, Belgium
email: georges.kouroussis@umons.ac.be

Antonio Romero, Pedro Galvín
Universidad de Sevilla, Escuela Técnica Superior de Ingeniería, Sevilla, Spain

David P. Connolly
The University of Leeds, Institute for High Speed Rail, Leeds, UK

Railway-induced ground-borne vibration is an undesirable nuisance affecting residents close to railway lines. Although invariant properties are assumed along the longitudinal direction of the track for most typical problems (high-speed lines, metro lines, etc), this hypothesis is invalid for the case of localized defects (e.g. rail joint or turnout, usually encountered on urban networks). Ground vibrations of this form are the result of the interactions between the railway vehicle and track defects. At low vehicle speed (e.g. light transit vehicles, like trams or metros), the dynamic track deflection dominates the ground wave generation meaning that the quasi-static excitation (moving load effect) can be neglected. It is therefore reasonable to consider a single force acting at the wheel/rail defect contact point as the only source of railway vibration. Based on this consideration, a fast approach is described, which combines the time domain simulation of vertical wheel-defect contact, with track/soil transfer functions in the wavenumber-frequency-domain. The latter is defined using a 2.5D coupled finite element/boundary element (FE/BE) model for the track/soil. The effect of defect type and train speed is investigated.

Keywords: urban area, rail joint, ground vibration, scoping approach, 2.5D FE/BE model

1. Introduction

Numerous environmental technical challenges are associated to railway infrastructure, including the assessment of urban railway vibrations. A detailed evaluation of mitigation methods dedicated to track and soil systems was recently conducted in [1], with the aim of life-cycle performance analysis. To understand the nature of railway ground waves and their associated characteristics, prediction models are unavoidable. Figure 1 indicates the major source of vibration originating from the passing of trains. In addition to the moving load effect, track and wheel surface imperfections generate additional vibrations. Most often, complete numerical prediction models includes some of these effects (e.g. track rail joint [2], wheel flat [3]).

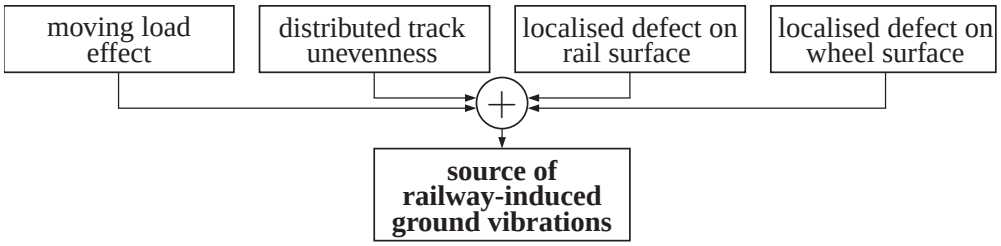

Figure 1: Cumulative effect of different sources of railway-induced ground vibrations.

Compared to other forms of railway network, urban area impose some technical track sections, e.g. turnouts, rail joints, switches, foundation transition, crossing, deducing that the main contribution in urban railroad is the dynamic excitation born in the wheel/rail contact. This explains why much of research has been recently performed in this area [4–9]. The behaviour of the soil and the subgrade also plays an important role [10]. As shown in Figure 2, the complexity in a prediction model involves some conditions: the vehicle/track and the track/soil interaction imposes some numerical constraints [11]. In addition, building amplifies the vibration levels in some specific structural frequencies [12]. Vehicle/track/soil/building interaction needs ideally to be modelled using multiple, yet coupled, sub-domains.

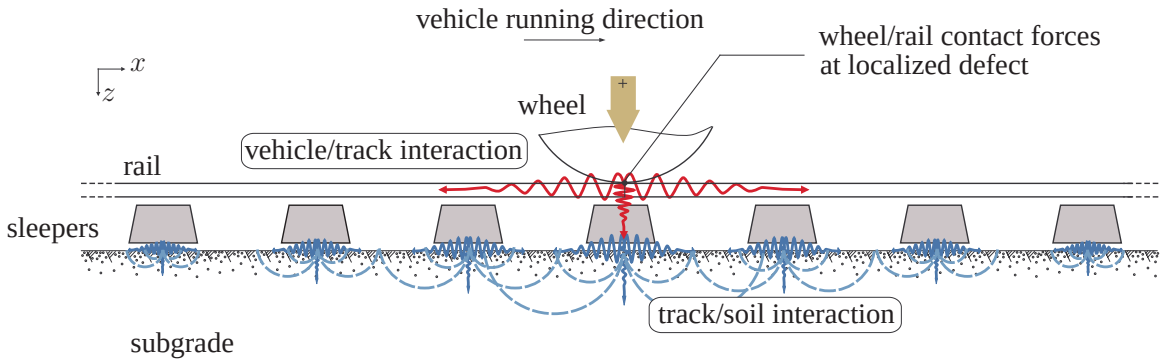

Figure 2: Wheel/rail and sleeper/subgrade interactions.

In [13], a model was presented, based on a rapid calculation of the wheel/rail forces and track/soil transfer functions in a separate way. This provides only the dynamic contribution of a localized defect on track surface, without considering the moving load effect. This was based on a previous approach, involving experimental data for the transfer functions [14, 15]. A first validation was proposed in [13], showing the high potential of the proposed approach, compared to more complete and rigorous developments [16, 17]. The aim of this paper is to complete [13] by presenting additional validating results and the possible types of results obtained, including the effect of defect type and train speed.

2. Basic concepts of the proposed prediction model

The proposed prediction model is based on two successive calculations. Complexity required the problem to be split. This approach allows the most well-suited modelling approach to be used for each subsystem (Figure 3):

- Step 1 is based on coupled multibody/finite element models allowing a realistic assessment of the wheel/rail force acting during the contact of a localized defect. This subdomain is a part of the

prediction scheme proposed in [18]. Bounce and pitch motions of car bodies and bogies are taken into account in the vehicle modelling. The track is defined by a rail modelled by an Euler- Bernoulli beam, discretely supported by the sleepers. Railpads and ballast are represented by spring and damper elements. The vehicle/track coupling is defined using the Hertzian law where any kind of surface track artefacts can be included such as switches, crossings, joints and changes in rail height. The vehicle speed v_0 is assumed to be constant. The wheel/rail contact forces are calculated

$$F_{\text{wheel/rail},n} \quad = \quad K_{Hz} \left(z_{\text{wheel,n}} - z_{\text{rail}}(x_j) - h_{\text{defect}} \right)^{3/2} \tag{1}$$

where $z_{\text{wheel,n}}$ is the vertical position of the n^{th} wheel and $z_{\text{rail}}(x_j)$ the vertical displacement at the rail at coordinate x_j. K_{Hz} is the Hertz's coefficient and h_{defect} the geometry of the imposed defect. A pre-processing step is used to solve the three-dimensional contact problem and to tabulate the different values of K_{Hz} as a function of the wheel position with respect to the defect shape, before considering the contact stiffness. The forces from Eq. (1) act at the defect location and are more accurate when taking into account the track/foundation flexibility and are saved as inputs of the evaluation process. In this case, the discrete Fourier transform (DFT) is used to calculate the frequency content $F_j(f)$ of the wheel/rail contact force set at the defect location.

- Step 2 provides the point source transfer function between the defect location and any point of the soil surface. A 2.5D finite element/boundary element (FE/BE) model is used to predict the track and free field vibrations [19]. A domain decomposition method is used to solve the problem, separating the track and the soil in different subdomains. The soil is modelled as a horizontally layered half-space. FE and BE are coupled by imposing equilibrium of forces and compatibility of displacements at the interface between both subdomains. The equilibrium equation for the dynamic soil-track interaction problem is formulated in a variational form [20]. A DFT is then applied to obtain the transfer mobility functions $M_{ij}(f)$ at different receiver locations i.

Combining step 1 and step 2 results, the velocity response is finally obtained

$$V_i(f) = M_{ij}(f) F_j(f) \tag{2}$$

in the frequency domain. An inverse Fourier transform then allows for time history representation.

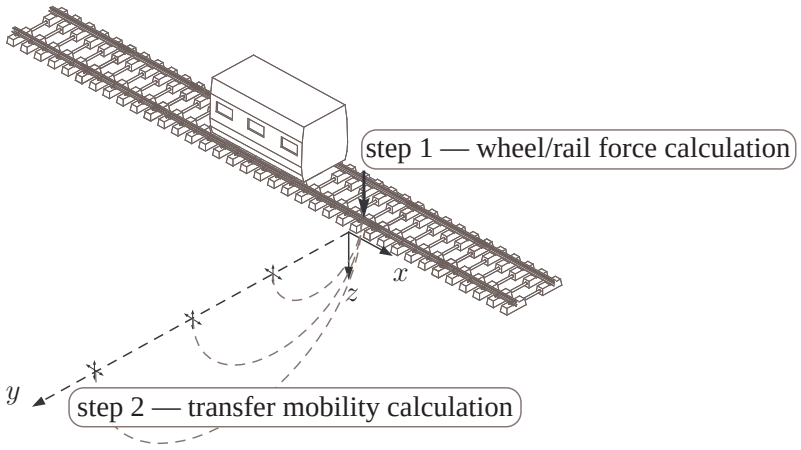

Figure 3: Modelling approach for ground vibration from local sources of excitation.

3. Model validation

The proposed validating case is based on a $125\,\mathrm{km/h}$ intercity train (AM96) passing over a track with a localised defect. The vehicle consists of 2×3 similar cars with articulated bogies. The leading wagon is equipped with motorized bogies. The track is a classical ballasted track with an embankment (L161 line in Brussels, Belgium). Vehicle, track and soil configuration are given in detail in [2]. The considered defect is a rail joint, modelled as a positive pulse of height h of $1\,\mathrm{mm}$ and a length l of $6\,\mathrm{mm}$. To model the analytical expression h_{defect} related to this shape, the vehicle wheel radius is taken into account.

Figure 4 presents the results obtained with the proposed simplified approach. The passing of each wheelset is visible on these trace velocities. In addition, two additional datasets are presented: one obtained from a complete model (Figure 5), taking into account all the sources of vibration, including the moving load effect, but requiring excessive CPU time; and the other one related to experiments presented in [2] (Figure 6). A similar shape is obtained, with maximum amplitude agreement, validating also the hypothesis of wheel/rail interaction force at localized defects as the main contributor to ground vibration in the presented case. Compared to the complete simulation (which includes a 3D FE representation of the ground wave propagation), the proposed model needs a few hours of CPU time (instead of a few days).

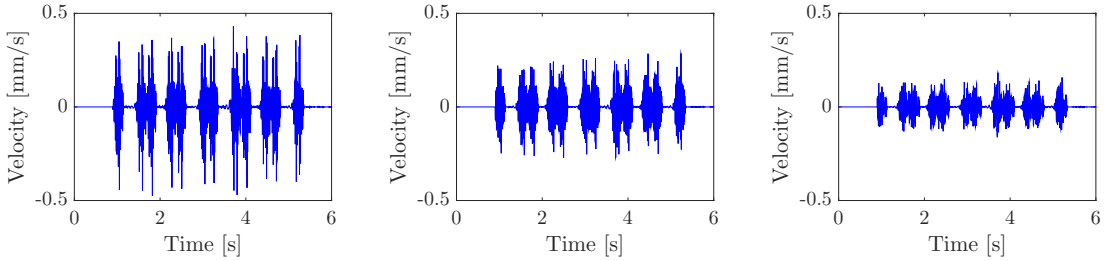

(a) At $14\,\mathrm{m}$ (b) At $18\,\mathrm{m}$ (c) At $22\,\mathrm{m}$

Figure 4: Time history at different distances from the track generated by an AM96 train running at $125\,\mathrm{km/h}$ a track with a localised defect: results obtained with the proposed simplified approach.

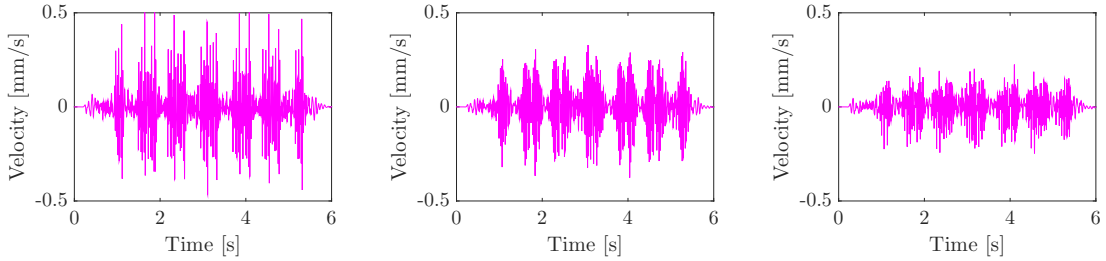

(a) At $14\,\mathrm{m}$ (b) At $18\,\mathrm{m}$ (c) At $22\,\mathrm{m}$

Figure 5: Time history at different distances from the track generated by an AM96 train running at $125\,\mathrm{km/h}$ a track with a localised defect: results obtained with the complete method described in [2].

Figure 7 presents peak particle velocity and root mean square values as a function of the distance from the track. In addition to the data collected during an experimental campaign (red line), additional results are presented, obtained from complete method: one with all the sources of vibrations (Figure 5), one without considering the localized defect (called static contribution) and one obtained by subtracting the

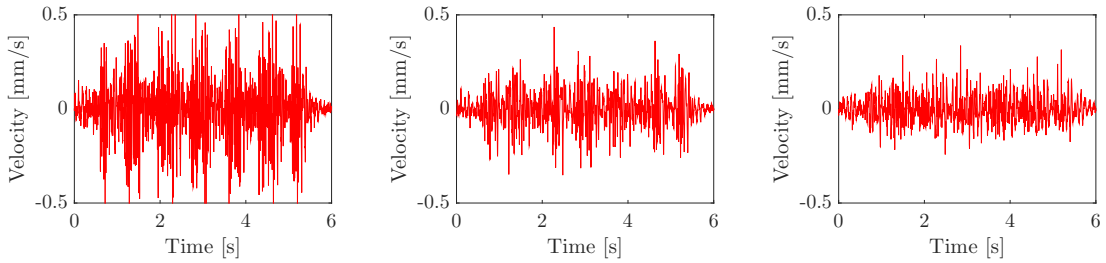

(a) At 14 m (b) At 18 m (c) At 22 m

Figure 6: Time history at different distances from the track generated by an AM96 train running at 125 km/h a track with a localised defect: experimental results presented in [2].

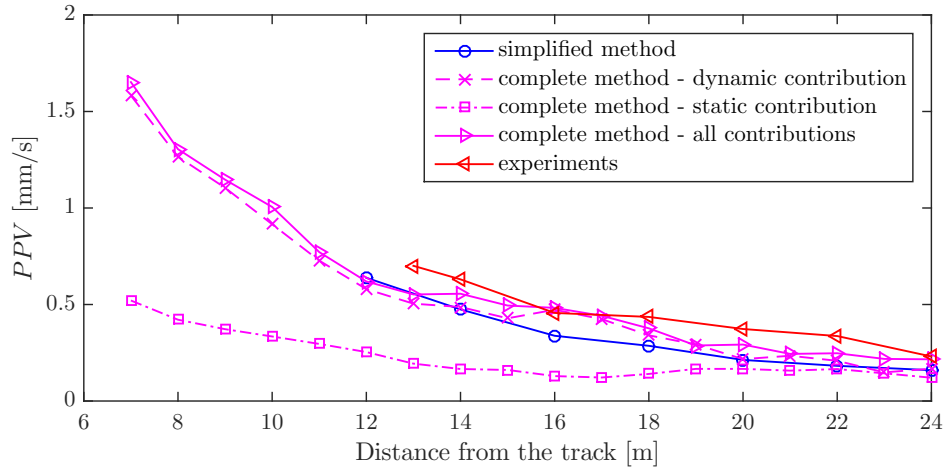

(a) Peak particle velocity

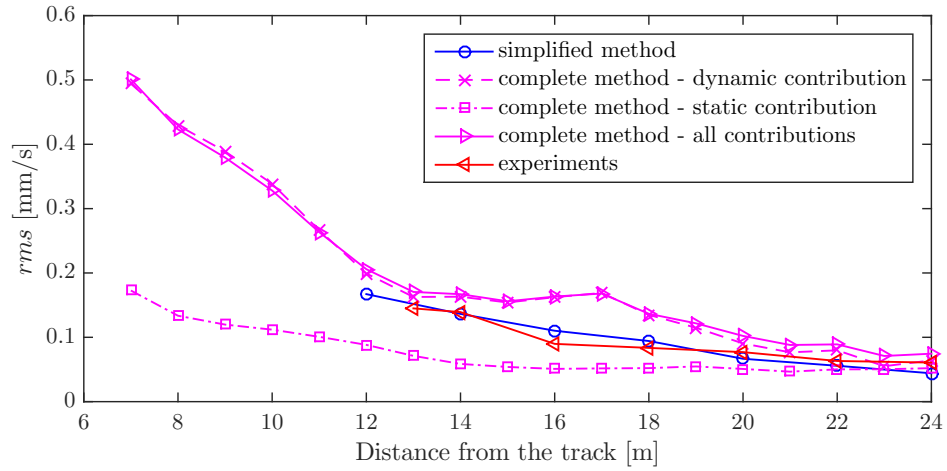

(b) Root mean square values

Figure 7: Numerical and field measured results level versus distance from track.

static contribution to the all the contributions in order to obtain the same working hypothesis than those from the simplified model (called dynamic contribution). The results show that the correlation between the proposed simplified model and the field measurement is acceptable. Moreover, it is shown that the

moving load effect is negligible compared to the dynamic effect generated by a wheel the passing over a localized defect. This point is relevant because it validates the assumption that underpins the proposed simplified model.

4. Sensitivity analysis

Two sets of analysis are performed. The first is into the effect of defect type on ground-borne vibration. The second is into the effect of train speed on ground-borne. The same track and soil configuration than previous section is retained. Figure 8 presents the four kinds of shape retained in this analysis. The values of defect length l and height h were selected according to those found in practice ($l = 125\,\mathrm{mm}$ and $h = 1\,\mathrm{mm}$).

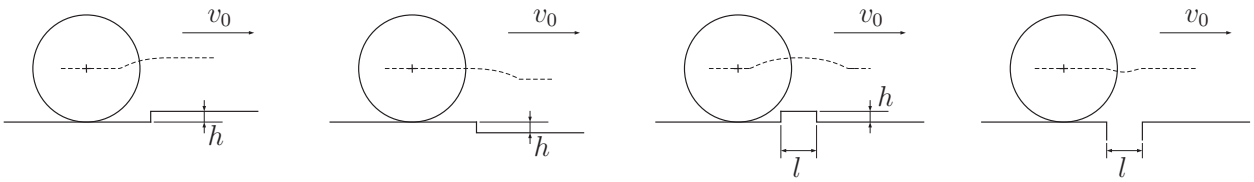

(a) Step-up joint (b) Step-down joint (c) Pulse (d) Negative pulse

Figure 8: Mathematical modelling of singular rail and wheel surface defects.

Figure 9 presents the level of surface ground vibrations induced by these different defect shapes at various distances from the track. Although there is similarity between the studied defects and dimensions, the presented results show some discrepancies between ground vibration levels. More particularly, a difference of results is obtained between the step-up and step-down joint cases, even if the geometry is symmetrically identical. This is due to the non-linear effects at the wheel/rail contact where climbing and dropping do not represent the same dynamic effect. Higher values for positive pulse are also observed, due to the cumulative effect of step-up and step-down functions defining the positive pulse. Finally, the decrease of level with the distance is not identical for each defect; different decreasing rates and some small local increases in PPV are seen with the distance.

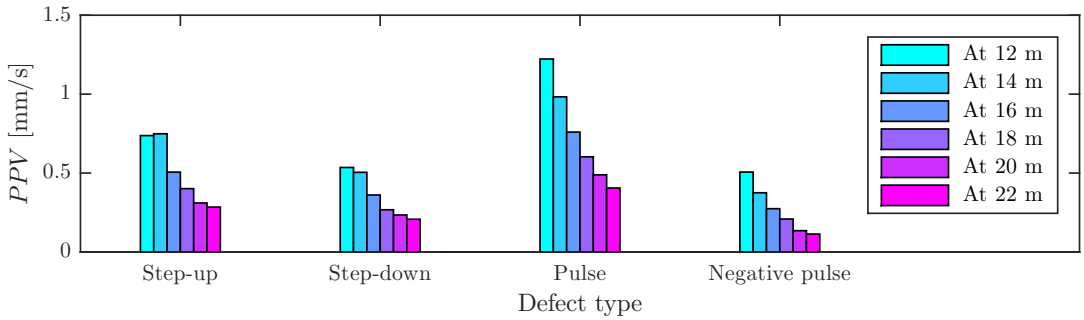

Figure 9: Peak particle velocity as a function of the distance from the source and the defect type for an AM96 trainset running at $120\,\mathrm{km/h}$.

Figure 10 presents the variation in ground vibration level with the speed, from 60 to $150\,\mathrm{km/h}$, considering the negative pulse. It is shown that there is no strong positive effect of speed on ground vibration level, as usually observed for the moving load effect. Although track displacements typically increase with train speed (e.g. critical velocity), here, the lowest speed ($60\,\mathrm{km/h}$) generates the highest peak response. This is because the vehicle eigenmodes that contribute to the vehicle/track interaction

forces when passing over a singular defect are dominant, independently of the vehicle speed, with the effective non-linearity on the defect contact.

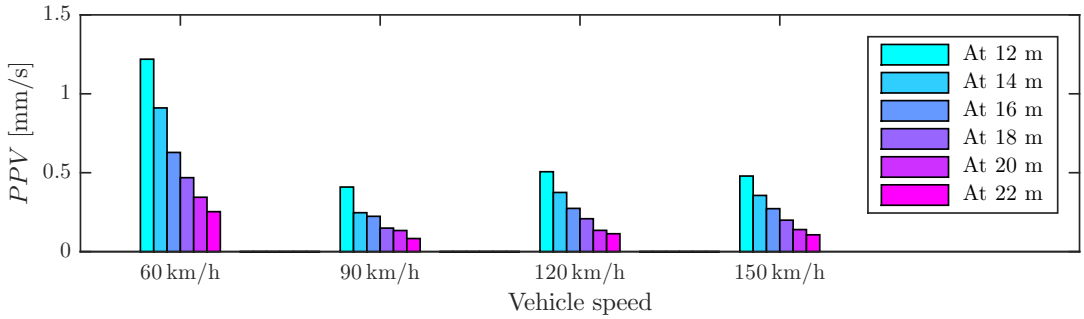

Figure 10: Peak particle velocity as a function of the distance from the source and the train speed for an AM96 trainset running on a negative pulse.

5. Conclusion

A rapid computation approach was proposed in this paper to evaluate the impact of localized rail surface defect on neighbour environment. A distinction between the static contribution (moving load effect) and the dynamic contribution (interaction between the vehicle and the rail defect) of the passing of a railway vehicle allowed the establishment of a 2-step simulation taking into account the interaction of rail vehicles with a singular defect: each of these steps provides an independent information to calculate the resulting ground vibration. The numerical results were validated with experimental data and other numerical data provided by a complete simulation model. This shows that accurate results can be obtained even if the attention is only paid on the dynamic effect of localised defects.

Acknowledgement

The research about the track/soil system was funded by the Spanish Ministry of Economy and Competitiveness (Ministerio de Economía y Competitividad) through research project BIA2016-75042-C-1-R2. Financial support is gratefully acknowledged. The support given by the Andalusian Scientific Computing Centre (CICA), the University of Leeds Cheney Award Scheme and the Leverhulme Trust (UK) is also gratefully.

REFERENCES

1. Kaewunruen, S. and Martin, V. Life cycle assessment of railway ground-borne noise and vibration mitigation methods using geosynthetics, metamaterials and ground improvement, *Sustainability*, **10** (10), 3753, (2018).

2. Kouroussis, G., Florentin, J. and Verlinden, O. Ground vibrations induced by intercity/interregion trains: A numerical prediction based on the multibody/finite element modeling approach, *Journal of Vibration and Control*, **22** (20), 4192–4210, (2016).

3. Alexandrou, G., Kouroussis, G. and Verlinden, O. A comprehensive prediction model for vehicle/track/soil dynamic response due to wheel flats, *Journal of Rail and Rapid Transit*, **230** (4), 1088–1104, (2016).

4. Vogiatzis, K. and Kouroussis, G. Prediction and efficient control of vibration mitigation using floating slabs: Practical application at Athens metro lines 2 and 3, *International Journal of Rail Transportation*, **3** (4), 215–232, (2015).

5. Germonpré, M., Degrande, G. and Lombaert, G. Periodic track model for the prediction of railway induced vibration due to parametric excitation, *Transportation Geotechnics*, **17**, 98–108, (2018).

6. Talbot, J. P. Lift-over crossings as a solution to tram-generated ground-borne vibration and re-radiated noise, *Journal of Rail and Rapid Transit*, **228** (8), 878–886, (2014).

7. Kliukas, R., Jaras, A. and Kacianauska, R. Investigation of traffic-induced vibration in Vilnius arch-cathedral belfry, *Transport*, **23** (4), 323–329, (2008).

8. Kouroussis, G., Connolly, D. P., Vogiatzis, K. and Verlinden, O. Modelling the environmental effects of railway vibrations from different types of rolling stock — a numerical study, *Shock and Vibration*, **Vol. 2015** (article ID 142807), 16 pages, (2015).

9. Zhu, S., Yang, J., Cai, C., Pan, Z. and Zhai, W. Application of dynamic vibration absorbers in designing a vibration isolation track at low-frequency domain, *Proceedings of the Institution of Mechanical Engineers, Part F: Journal of Rail and Rapid Transit*, **231** (5), 546–557, (2017).

10. Kouroussis, G., Connolly, D. P., Olivier, B., Laghrouche, O. and Alves Costa, P. Railway cuttings and embankments: experimental and numerical studies of ground vibration, *Science of the Total Environment*, **557-558**, 110–122, (2016).

11. Kouroussis, G. and Verlinden, O. Prediction of railway ground vibrations: accuracy of a coupled lumped mass model for representing the track/soil interaction, *Soil Dynamics and Earthquake Engineering*, **69**, 220–226, (2015).

12. Mouzakis, H. and Vogiatzis, K. Ground-borne noise and vibration transmitted from subway networks to multi-storey reinforced concrete buildings, *Transport*, **33** (2), 446–453, (2018).

13. Kouroussis, G., Olivier, B., Romero, A., Galvín, P. and Connolly, D. P. A fast numerical assessment of railway-induced ground vibration in urban conditions, *Proceedings of the 25th International Congress on Sound and Vibration*, Hiroshima (Japan), (2018).

14. Kouroussis, G., Vogiatzis, K. E. and Connolly, D. P. A combined numerical/experimental prediction method for urban railway vibration, *Soil Dynamics and Earthquake Engineering*, **97**, 377–386, (2017).

15. Kouroussis, G., Vogiatzis, K. and Connolly, D. P. Assessment of railway ground vibration in urban area using in-situ transfer mobilities and simulated vehicle-track interaction, *International Journal of Rail Transportation*, **6** (2), 113–130, (2018).

16. Kouroussis, G., Connolly, D. P., Alexandrou, G. and Vogiatzis, K. The effect of railway local irregularities on ground vibration, *Transportation Research — Part D: Transport and Environment*, **39**, 17–30, (2015).

17. Kouroussis, G., Connolly, D. P., Alexandrou, G. and Vogiatzis, K. Railway ground vibrations induced by wheel and rail singular defects, *Vehicle System Dynamics*, **53** (10), 1500–1519, (2015).

18. Kouroussis, G., Van Parys, L., Conti, C. and Verlinden, O. Prediction of ground vibrations induced by urban railway traffic: an analysis of the coupling assumptions between vehicle, track, soil, and buildings, *International Journal of Acoustics and Vibration*, **18** (4), 163–172, (2013).

19. François, S., Schevenels, M., Galvín, P., Lombaert, G. and Degrande, G. A 2.5D coupled FE-BE methodology for the dynamic interaction between longitudinally invariant structures and a layered halfspace, *Computer Methods in Applied Mechanics and Engineering*, **199** (23), 1536–1548, (2010).

20. Galvín, P., François, S., Schevenels, M., Bongini, E., Degrande, G. and Lombaert, G. A 2.5D coupled FE-BE model for the prediction of railway induced vibrations, *Soil Dynamics and Earthquake Engineering*, **30** (12), 1500–1512, (2010).